C.P. No. 761

C.P. No. 761

MINISTRY OF AVIATION

AERONAUTICAL RESEARCH COUNCIL

CURRENT PAPERS

Flutter Calculations on a Body with Aft Wings

by

E. G. Broadbent and E. V. Hartley

LONDON: HER MAJESTY'S STATIONERY OFFICE

1964

PRICE 5s 6d NET

U.D.C. No. 533.6.013.422 : 629.19.012.674

C.P. No.761

August, 1963

FLUTTER CALCULATIONS ON A BODY WITH AFT WINGS

by

E.G. Broadbent
and
E.V. Hartley

SUMMARY

The effect of body flexibility on the flutter of a body with aft wings is investigated. The missile is in free supersonic flight and the wings are assumed rigid in torsion. It is found that flutter can occur either between wing bending and the rigid body modes, or between wing bending and the fundamental bending mode of the body, depending on body stiffness. If the latter form of flutter is possible (as it usually is in practice) a higher wing stiffness is required for its avoidance. A close approximation to the quaternary flutter solution in this case is given by the appropriate binary calculation. The flutter is fairly sensitive to parameters that affect the static margin (Mach number and c.g. position) and also to structural damping.

Replaces R.A.E. Technical Note No. Structures 337 - A.R.C. 25,214.

CONTENTS

		Page
1	INTRODUCTION	4
2	MODES OF DEFORMATION AND STRUCTURAL ASSUMPTIONS	4
3	AERODYNAMIC ASSUMPTIONS	6
4	SOLUTION OF THE FLUTTER EQUATIONS	7
5	RESULTS AND CONCLUSIONS	9
	5.1 The basic calculation	9
	5.2 The effect of an extra body mode	12
	5.3 Variation of physical parameters	12
	5.4 Conclusions	13
SYMBOLS		13
REFERENCE		15
APPENDIX 1 - The flutter equation and numerical coefficients		16
TABLES 1-5		-
ILLUSTRATIONS - Figs.1-9		-
DETACHABLE ABSTRACT CARDS		-

TABLES

Table			
1	-	Static margins of stability at different Mach numbers	7
2	-	Assumed geometry of body	8
3	-	Flutter coefficients in 4 degrees of freedom	18
4	-	Normal mode binary from quaternary	20
5	-	Normal mode ternary from quinary	21

ILLUSTRATIONS

	Fig.
Plan view of configuration chosen	1
Typical flutter boundary (M = 4) and comparison with a binary result	2
Flutter boundaries for five Mach numbers	3
The first two normal modes of the body	4
Effect of the second body mode on the binary flutter boundary	5
Effect of c.g. variations on the flutter boundaries	6
Effect of body mass on the flutter boundaries	7
Effect of structural damping on the flutter boundaries	8
Typical flutter boundary showing two points of known instability	9

1 INTRODUCTION

It is known that a body with aft wings (or fins) can suffer from body freedom flutter, i.e. an unstable oscillation involving pitch, heave and wing bending. The present investigation was carried out to see whether flexibility of the body had a major effect on the flutter. The writers expected that it might do so since body bending could replace pitch and heave, and because of the higher frequency involved, a higher wing stiffness for flutter prevention would be required. This result was in fact borne out by the calculations.

The basic calculation included four modes, (1) heave, (2) pitch, (3) body bending and (4) wing bending. The parameters varied were (1) Mach number (using piston theory on the wing) and (2) c.g. position, and the results are presented in graphic form, plotting the wing bending stiffness against body bending stiffness for a given critical speed. The calculations were later extended to include the effect of one overtone body mode; this extra mode was not important for the configuration selected.

2 MODES OF DEFORMATION AND STRUCTURAL ASSUMPTIONS

It is known that classical body freedom flutter of bodies with aft wings is possible with the three degrees of freedom, heave, pitch and wing bending. The intention in this paper is to investigate the change in this basic body freedom flutter when body bending is also included. The first part of the investigation was carried out by representing body bending by one degree of freedom.

The missile considered is shown in Fig.1*. In view of the general nature of the investigation it was decided to assume a uniform mass distribution from nose to tail, the wing being included with the aft part of the body; there will obviously be departures from this in practice but not, it is thought, of a serious nature. The body stiffness distribution was also assumed uniform and on the wing the mass per unit area was assumed uniform. The numerical values of these assumed mass distributions are given later in Table 2 on Page 8, but it is apparent that the assumption of uniform overall mass distribution from nose to tail implies that the mass per unit length of the body alone falls near the tail, and in fact at the extreme tail it has fallen to about 89% of the value ahead of the wing. The c.g. was thus at a distance $\frac{1}{2}\ell$ from the nose where ℓ is the total length of the body, and this point is taken as the origin of coordinates in the analysis which follows. The rigid modes, heave and pitch about the c.g. are defined by

$$\frac{z}{\ell} = q_1 + \xi\, q_2$$

where z is vertical displacement

---

*The term missile is appropriate to the type of planform selected, although this was not based on any specific missile, military or otherwise.

$\xi = \frac{x}{\ell}$

x is the distance of a point aft of the c.g.

q_1 is the generalised coordinate of heave

q_2 is the generalised coordinate of pitch.

Since the mass and structural distributions are assumed uniform over the whole length of the weapon, the bending modes of the body will be symmetric or antisymmetric about the origin, and any one bending mode will therefore contain either even powers of ξ or odd powers of ξ but not both. The fundamental mode, which it is desired to represent in the first place, will be symmetric about the origin and so will contain only even powers of ξ. The end conditions of zero bending moment are satisfied by $\frac{\partial^2 z}{\partial \xi^2}$ tending to zero at the nose and tail. The symmetric body bending mode is therefore defined by

$$\frac{z}{\ell} = (1.5\,\xi^2 - \xi^4)\, q_3$$

where q_3 is the generalised coordinate of body bending.

It is also assumed that the curvature of this bending mode continues outwards along the wing span, giving wing camber deformation entirely dependent on body bending. It is likely that this assumption is not true in practice, but the body curvature at the ends of the body is small and there will therefore be little camber effect to include in the calculations. In addition, the wings are highly tapered, and this reduces the likelihood of there being any important camber change associated with wing bending.

The assumption that the wing bending is parabolic spanwise is made. This mode implies that the ratio of the bending moment to bending rigidity tends to a finite quantity at the wing tips since the curvature does not fall to zero. This is quite possible with pointed tips. The wing bending mode is therefore defined by

$$\frac{z}{\ell} = \eta^2\, q_4$$

where $\eta = \frac{y}{\ell}$

y is the spanwise coordinate

q_4 is the generalised coordinate of wing bending.

The complete deformation of the missile is thus defined by

$$\frac{z}{\ell} = q_1 + \xi\, q_2 + (1.5\,\xi^2 - \xi^4)\, q_3 + \eta^2\, q_4 \quad . \qquad (1)$$

The structural stiffnesses were not evaluated by integration of the strain energy since only two modes are involved and the two stiffnesses are uncoupled; instead the two generalised stiffnesses were treated as independent variables.

For the second part of the investigation it was decided to include the body mode of next higher order. This bending mode will contain only odd powers of ξ, and as the end conditions of zero bending moment are satisfied by $\frac{\partial^2 z}{\partial \xi^2}$ tending to zero at the nose and tail the mode is defined by

$$\frac{z}{\ell} = (\xi^3 - 1.2\,\xi^5)\, q_5$$

where q_5 is the second generalised coordinate of body bending.

As in mode three, the assumption is made that the body curvature continues outwards along the wing span, giving wing camber deformation entirely dependent on body bending.

The complete deformation of the weapon for the second part of the investigation is therefore defined by

$$\frac{z}{\ell} = q_1 + \xi\, q_2 + (1.5\,\xi^2 - \xi^4)\, q_3 + (\xi^3 - 1.2\,\xi^5)\, q_5 + \eta^2\, q_4 \quad . \qquad (2)$$

Because of the nature of modes 3 and 5, one being symmetric about the origin and the other antisymmetric, there is no elastic coupling between them. There is however one additional structural stiffness, E_{55}, and the ratio between E_{55} and E_{33} was calculated for a uniform beam.

The inertia coefficients were calculated from the kinetic energy appropriate to the equation for the displacement, e.g. equation (2). The two symmetric modes (1 and 3) are both orthogonal with each of the antisymmetric modes 2 and 4. It should perhaps be made clear that the term antisymmetric is used in the sense of antisymmetry about the c.g.; all the modes are, of course, symmetric in the usual sense of symmetry about a plane normal to the wings and through the centre-line.

3 AERODYNAMIC ASSUMPTIONS

The forces on the body were assumed negligible except over the conical nose and over this part of the body slender-body theory was used. The conical nose extends for 20% of the total length ℓ and the maximum diameter is 10% of

the total length. For the wing itself, second order piston theory (i.e. including first order thickness effects) was used. The maximum chord of the wing, adjacent to the body, is 0.2ℓ and the leading edge sweepback is 60°. The wing section is assumed to be a symmetric biconvex section with a constant thickness to chord ratio of 5%.

The Mach numbers considered were 1, 2, 3, 4 and 5 and the altitude 30,000 ft, although piston theory is clearly inapplicable at M = 1. The aerodynamic stiffness (e.g. lift and pitching moment due to wing incidence) are directly proportional to Mach number by piston theory whereas slender body theory gives forces proportional to M^2 on the nose. It follows that as Mach number is increased the static stability of the weapon is reduced, since the c.g. is kept fixed, and this fact should be kept in mind when considering the results. Positive stability is retained up to a Mach number of about $6\ 2/3$. The static margin at the different Mach numbers is given in Table 1 below.

TABLE 1

Static margins of stability at different Mach numbers

M	Static margin (% ℓ)
0	43.3
1	36.5
2	22.6
3	15.8
4	10.3
5	5.85

4 SOLUTION OF THE FLUTTER EQUATIONS

The equations are written in the form

$$[a\lambda^2 + b\lambda + c + e]\ q = 0 \qquad (3)$$

where a is the square matrix of inertia coefficients

b is the square matrix of aerodynamic damping coefficients

c is the square matrix of aerodynamic stiffness coefficients

e is the diagonal matrix of structural stiffness coefficients

q is the column of generalised coordinates.

The motion is of the form $q = \bar{q}e^{\lambda\tau}$, where

$$\tau = \frac{V_s\, t}{\ell} \quad .$$

Thus in the critical flutter condition

$$\lambda = \frac{i\omega\ell}{V_s}$$

where ω is the flutter frequency (rad/sec)

ℓ is the body length (ft)

V_s is the speed of sound (ft/sec).

The basic calculations assumed the data given below in Table 2.

TABLE 2

Assumed geometry of body

Symbol	Significance	Value
ℓ	length of body	25 ft
$2R_{max}$	body diameter	2.5 ft
Λ	wing sweep (leading edge)	60°
C_o	wing root chord	5 ft
	c.g. aft of nose	12.5 ft
m_b	mass per unit length of weapon	9.528 slugs/ft
μ_w	mass per unit area of wing	0.1842 slugs/ft^2
ρ	air density at 30,000 ft	0.889×10^{-3} slugs/ft^3
γ	ratio of specific heats	1.4

These data led to the flutter coefficients given in Table 3 in the Appendix for the first calculation in four degrees of freedom appropriate to equation (1). It may be noted that λ is based on a fixed speed so that the forward speed occurs directly in the aerodynamic coefficients which are functions of Mach number.

The structural stiffness matrix contains only two non-zero elements which represent the bending stiffness of the body and the wing. They are made non-dimensional by use of the speed of sound and are defined by

$$\left.\begin{aligned} x &= \frac{E_{33}}{\rho V_s^2 \ell^3} \\ y &= \frac{E_{44} \times 10^6}{\rho V_s^2 \ell^3} \end{aligned}\right\} \qquad (4)$$

where E_{33} and E_{44} are the dimensional stiffnesses based on the strain energy in a displacement of the type given by equation (1); i.e. the strain energy $\bar{V}$ is related to the coefficients by the equation

$$2\bar{V} = E_{33} q_3^2 + E_{44} q_4^2 \quad . \qquad (5)$$

In the expression for y the factor of 10^6 is introduced so that the numerical values of x and y shall be more nearly of the same order.

The method of solution was to expand the flutter determinant (i.e. the determinant of the square matrix in equation (3)) in terms of M, λ, x and y. The chosen value of M was then substituted and the resulting polynomial in λ split into two parts consisting of the even and odd powers of λ respectively. Since in the flutter condition λ is pure imaginary these two polynomials could be equated separately to zero to give a pair of linear bivariate equations in x and y for every chosen value of λ. Thus a curve of y against x could be plotted for each Mach number.

5 RESULTS AND CONCLUSIONS

5.1 The basic calculation

Solution of the flutter equations for the four basic degrees of freedom leads to the curve shown in Fig.2. Here y is plotted against x and the numbers alongside the curve refer to the appropriate value of the non-dimensional frequency $\omega\ell/V_s$ (= λ/i). The particular case plotted in Fig.2 is for M = 4 from the expansion of the determinant given as equation (A1) in the Appendix in terms of Mach number, via equation (A2) in which the appropriate Mach number (M = 4) has been substituted.

For large values of x, approximating to the case of a rigid body we find the well known body freedom flutter in which instability occurs at the chosen Mach number for values of y less than the asymptotic value (1.135 in this case). For smaller values of y (i.e. for very low wing bending stiffness) instability would already have occurred at a lower Mach number. In addition to this there occurs a large oval area of instability starting near the origin and extending well into the positive quadrant before finally running off to the left and forming the negative asymptote of the body freedom flutter. This implies that for body stiffnesses in the range given by $0 < x < 1.2$ a very much larger value

of y (wing stiffness) is needed to eliminate flutter. The two ends of the curve for $\lambda \to 0$ can be deduced from equation (A2). One solution is clearly $y = 0$ from the coefficient of λ^2, and then the coefficient of λ^3 shows that the curve tends to the point (-0.669, 0); from this point the instability extends to infinity in both directions along the x-axis corresponding to the fact that below this axis (y negative) there is no aerodynamic stiffness and a negative structural stiffness in the wing bending freedom. The other solution for $\lambda \to 0$ is given by $x = 0.098$, also from the coefficient of λ^2 in equation (A2). In this case the coefficient of λ^3 shows that the curve tends to the point (0.098, 0.603) and again at this point the instability suddenly extends to infinity (shown by the dotted line in Fig.2) in both directions parallel to the y-axis: in other words this is the limiting value of x (body stiffness) below which a divergent instability exists.

To give an idea of the physical meaning of the scales of x and y, it is simplest to think in terms of the relevant natural frequencies, i.e.

$$\left.\begin{aligned} \omega_3 = \sqrt{\frac{E_{33}}{A_{33}}} = \frac{V_s}{\ell}\sqrt{\frac{x}{a_{33}}} &= 65.4\sqrt{x} \\ &\equiv 10.4\sqrt{x} \text{ c.p.s.} \end{aligned}\right\} \quad (6)$$

$$\left.\begin{aligned} \omega_4 = \sqrt{\frac{E_{44}}{A_{44}}} = \frac{V_s}{1000\,\ell}\sqrt{\frac{y}{a_{44}}} &= 15.1\sqrt{y} \\ &\equiv 2.39\sqrt{y} \text{ c.p.s.} \end{aligned}\right\} \quad (7)$$

Of these, ω_3 is the natural frequency of the body in bending when clamped at its c.g., and ω_4 is the natural frequency of the wing clamped at the root.

The curves for all five Mach numbers are given in Fig.3, and it may be seen that the area of instability increases progressively with Mach number. To clear the oval area for M = 5, for example, requires (with a margin of about 15%) that

$$\left.\begin{aligned} &\text{either} && x > 1.6 \\ &\text{or} && y > 18 \end{aligned}\right\} \quad (8)$$

$$\left.\begin{aligned} &\text{i.e.} && \omega_3 > 13 \text{ c.p.s.} \\ & && \omega_4 > 10 \text{ c.p.s.} \end{aligned}\right\} \quad (9)$$

The similarity in the requirements for these two frequencies suggests that the oval area is caused by a frequency coincidence. The most likely explanation is

that the normal mode associated with body bending and the rigid body freedoms combines with wing bending to give binary flutter; the combination has some similarities with torsion and flexure in a conventional wing.

This binary calculation was now carried out. The coefficients of the binary equations are given in Table 4 of the Appendix. The structural stiffness of the normal mode is directly proportional to x and so the graph of y against x takes the well-known elliptic form (see Ref.1). The quadratic nature of the equation in x and y after eliminating λ arises as follows. Let the expansion of the determinant be

$$\Delta \equiv p_0 \lambda^4 + p_1 \lambda^3 + p_2 \lambda^2 + p_3 \lambda + p_4 \quad . \tag{10}$$

Then p_0 and p_1 are independent of x and y; p_2 and p_3 are linear in x and y and p_4 contains the product xy. It follows from equating the odd powers of λ to zero that λ^2 is linear in x and y, and hence the equation

$$p_0 \lambda^4 + p_2 \lambda^2 + p_4 = 0 \tag{11}$$

yields a quadratic in x and y that turns out to be an ellipse, and since the constant term in the equation in x and y is very small, the ellipse passes close to the origin. The agreement between the normal mode binary calculation*, and the oval part of the quaternary solution is quite striking as can be seen from Fig.2. Part of the ellipse for negative values of x relates to negative values of λ^2.

The values of x and y bounding the binary ellipse with a 15% margin are, for a Mach number of 4,

$$x = 1.274$$

$$y = 15.15$$

compared with the quaternary values of 1.257, and 14.55, respectively. The comparison in terms of frequency is

$$\bar{\omega}_3 = 18.1 \text{ (cf. 11.7 c.p.s.)}$$

$$\bar{\omega}_4 = 9.30 \text{ (cf. 9.12 c.p.s.)}$$

---

*This description is used to distinguish the calculation from any possible binaries taken directly from the larger matrices of flutter coefficients. What has been done, however, is simply to normalise the first of the two modes with respect to pitch and heave; the two constituent modes in the binary calculation are not orthogonal to each other.

where $\bar{\omega}_3$, $\bar{\omega}_4$ are the natural frequencies of the two modes in the binary calculation. Since the frequency $\bar{\omega}_3$ relates to a body mode that is normal with respect to pitch and heave it is considerably higher than ω_3.

5.2 The effect of an extra body mode

An extra body mode, corresponding to overtone bending as given in Section 2 was now included. Solutions to the complete quinary calculation were not obtained. Instead the normal mode ternary was formed by first calculating the two normal modes from the two body freedoms and the two body bending modes, and then transforming the quinary by an appropriate matrix multiplication. The coefficients of this ternary are given in Table 5 in the Appendix and the two normal modes are shown in Fig.4. In fact it was found that the additional mode had little affect of the flutter solutions, and Fig.5 shows a plot of the oval obtained from this ternary calculation compared with the normal mode binary for the same case (M = 5). The reason for this is probably that the second body mode has a mode in the region of the wing.

5.3 Variation of physical parameters

The variations made were of c.g. position, body mass and structural damping. The c.g. position was varied by keeping the total mass constant and also the moment of inertia about the c.g. Four c.g. positions were taken, given by $\bar{\xi}$ = -0.04; -0.02; 0; 0.02 for M = 5. For each case the ellipse corresponding to the normal mode binary was calculated and the four curves are shown on Fig.6 with the quaternary ovals for $\bar{\xi}$ = 0 and -0.04 for comparison. The effect of this variation is to increase the size of the ellipse as the c.g. is moved aft, i.e. as the static margin is reduced. A rather curious result was obtained by varying the c.g. position by adding a concentrated mass at the nose of the missile. This mass was chosen to give a c.g. of $\bar{\xi}$ = -0.04, but the resulting ellipse is much larger than that for $\bar{\xi}$ = -0.04 at constant overall mass and pitching inertia. It is therefore dangerous to generalise about the effect of c.g. position in a particular missile when it is not clear what body parameters are kept constant during the variation.

In view of this result the effect of separately changing the body mass was investigated. It was found that a reduction in body mass at a particular value of x = 0.14 increased the range of instability in terms of y. This result is shown in Fig.7, but it can be seen from Fig.6 that it has little general significance on the size of the ellipse. The small value of x was chosen as being fairly typical of current practice.

The same value of x was used to investigate the range of flutter in terms of y as structural damping was increased from zero. The results are shown in Fig.8. It can be seen that the damping in the body mode has a powerful effect but that the damping in the wing in unimportant.

A check on this result is given by the comparatively slow rate of growth of the unstable oscillations within the quaternary oval. Fig.9 shows the quaternary for M = 1, but in addition to the critical boundary corresponding to pure imaginary values of λ, two points are plotted for a prescribed rate of growth equivalent to -1% critical damping, in fact

$$\lambda = \sqrt{0.3}\,(0.01 + i) \quad . \qquad (12)$$

In a very violent flutter the two points would be closer to the boundary than those shown in Fig.9.

5.4 Conclusions

For a missile with aft wings (or fins) at supersonic speeds, flutter involving wing bending is possible either with the rigid body freedoms, or with the fundamental body bending mode. Prevention of the latter type of flutter by providing adequate wing stiffness is likely to be the overriding requirement in practice because the body stiffness is likely to be within the range of the quaternary oval - as shown in Fig.2. In as much as the oval arises through a frequency coincidence, it might be thought that the overtone body bending would demand an even higher wing bending stiffness; for the configuration used in the calculations, however, this was not so because of the aft nodal line, and the overtone mode had an insignificant effect. There may well be other configurations, of course, where higher wing stiffness would be needed to avoid flutter with an overtone mode. Reduction of static margin, either by increasing Mach number or by aft shift of c.g., increases the area of instability. In the case of c.g. shift, however, this is only true if the body mass and pitching inertia are maintained constant. It is perhaps unwise to attempt to relate the size of the ovals directly with static margin, since the result probably depends on how the margin is varied. The flutter is fairly sensitive to structural damping in the body.

SYMBOLS

$\bar{a}$ is the square matrix of aerodynamic inertia coefficients

$\hat{a}$ is the square matrix of structural inertia coefficients

$a = \bar{a} + \hat{a}$, the square matrix of inertia coefficients

b is the square matrix of aerodynamic damping coefficients

c is the square matrix of aerodynamic stiffness coefficients

e is the diagonal matrix of structural stiffness coefficients

q is the column of generalised coordinates

q_1 is the generalised coordinate of heave

q_2 is the generalised coordinate of pitch

q_3 is the generalised coordinate of body bending

SYMBOLS (Contd.)

q_4 is the generalised coordinate of wing bending

q_5 is the 2nd generalised coordinate of body bending

ω is the flutter frequency (rad/sec)

ℓ is the body length (ft)

V_s is the speed of sound (ft/sec)

$\lambda = \frac{i\omega\ell}{V_s}$ in the critical flutter condition (in general the motion is of the form $e^{\lambda\tau}$ where $\tau = V_s\, t/\ell$)

z is vertical displacement

$\bar{\xi}\ell$ is the distance of the c.g. aft of the datum

$2R_{max}$ is the diameter of body

Λ is the wing sweep (leading edge)

C_o is the wing root chord

m_b is mass per unit length of body

μ_w is mass per unit area of wing

ρ is air density at 30,000 ft

γ is ratio of specific heats

$\bar{V}$ is strain energy

$x = \frac{E_{33}}{\rho V_s^2 \ell^3}$ non-dimensional bending stiffness of body

$y = \frac{E_{44} \times 10^6}{\rho V_s^2 \ell^3}$ non-dimensional bending stiffness of wing

ω_r is the natural frequency of the rth mode

$\bar{\omega}_r$ is the natural frequency of the corresponding normalised mode.

REFERENCE

No.	Author	Title, etc.
1	Fraser, R.A. Duncan, W.J.	The flutter of aeroplane wings. Aeronautical Research Council R & M No. 1155 August, 1928.

APPENDIX 1

THE FLUTTER EQUATION AND NUMERICAL COEFFICIENTS

The expanded form of the flutter equation is given in equation (A1) below. The motion is of the form $e^{\lambda\tau}$, where τ is proportional to time, and the Mach number M, and the two stiffnesses x and y are retained as variables in the equation. For a particular missile x and y would be fixed and for each value of M there would be various solutions for λ corresponding to the various stability roots. For the purposes of this paper, however, it is much more convenient to select values of λ and M and to solve for x and y, as explained in the main text.

$$
\begin{aligned}
0 \;=\; & \lambda^8\{8.5057468\} \\
& + \lambda^7\{2.11976694 + 0.00658227M\} \\
& + \lambda^6\{0.01615851 + 0.23947519M - 0.05102687M^2 + 54.62217957x + 3.86400452y\} \\
& + \lambda^5\{0.00000326 + 0.05742770M - 0.01198157M^2 - 0.00000179M^3 \\
& \qquad + (13.45327683 + 0.04913495M)\,x + (0.05700705 + 0.0026984 4M)\,y\} \\
& + \lambda^4\{(0.000326 - 0.000551M - 0.107388M^2 + 0.003295M^3)\,M10^{-2} \\
& \qquad + (0.06520413 + 0.44630536M - 0.11555314M^2)\,x \\
& \qquad + (0.00001328 + 0.2030631M - 0.02314961M^2)\,y + 24.48572114xy\} \\
& + \lambda^3\{(0.00454 - 0.25912M - 0.00622M^2)\,M^2 10^{-3} \\
& \qquad + (0.00000117 + 0.10485429M - 0.02760308M^2 - 0.00000056M^3)\,x \\
& \qquad + (0.1323 - 0.8422M + 0.0007M^2)\,My10^{-4} \\
& \qquad + (0.21641257 + 0.02154012M)\,xy\} \\
& + \lambda^2\{(0.01844 - 0.90431M + 0.01485M^2)\,M^2 y10^{-3} \\
& \qquad + (0.00000474 + 0.34328437M - 0.05147437M^2)\,xy\} \qquad \text{(A1)}
\end{aligned}
$$

Some of the properties of this equation can be more clearly seen after substitution for M, and the result for M = 4 reduces to

$$
\begin{aligned}
0 \;=\; & \lambda^8\{8.5057457\} \\
& + \lambda^7\{2.1460960\} \\
& + \lambda^6\{0.1576293 + 54.6221796x + 3.8640045y\} \\
& + \lambda^5\{0.0378943 + 13.6498167x + 0.06780080y\} \\
& + \lambda^4\{-\,0.0603677 + 0.00157538x + 0.4418719y + 24.4857212xy\} \\
& + \lambda^3\{-\,0.01491620 - 0.0222661x - 0.001252967y + 0.30257304xy\} \\
& + \lambda^2\{-\,0.05378002y + 0.5495522xy\} \qquad \text{(A2)}
\end{aligned}
$$

Tables 3, 4 and 5 give the numerical values of the flutter coefficients for various cases described in the main text. In Table 3 the matrices of the different types of coefficient are given separately, whereas Tables 4 and 5 each consist of the complete flutter matrix for the normal mode binary and ternary respectively, although in Table 4 the Mach number is left variable.

TABLE 3

Flutter coefficients in 4 degrees of freedom

$\bar{a}$ = the aerodynamic contribution to the total inertia coefficients

$$= 10^{-3} \begin{bmatrix} 0.5235988 & -0.1832596 & 0.0889145 & 0 \\ -0.1832596 & 0.0649262 & -0.0318247 & 0 \\ 0.0889145 & -0.0318247 & 0.0157318 & 0 \\ 0 & 0 & 0 & 0 \end{bmatrix}$$

$\hat{a}$ = the structural contribution to the total inertia coefficients

$$\begin{bmatrix} 17.140779773 & 0 & 1.928337747 & 0.42527244 \\ 0 & 1.428398284 & 0 & 0.19562532 \\ 1.928337747 & 0 & 0.374742087 & 0.11607143 \\ 0.42527244 & 0.19562532 & 0.11607143 & 2.26811953 \end{bmatrix}$$

$a = \bar{a} + \hat{a}$

$$\begin{bmatrix} 17.1413033718 & -0.1832596.10^{-3} & 1.9284266615 & 0.42527244 \\ -0.1832596.10^{-3} & 1.4284632102 & -0.0318247.10^{-3} & 0.19562532 \\ 1.9284266615 & -0.0318247.10^{-3} & 0.3747578188 & 0.11607143 \\ 0.42527244 & 0.19562532 & 0.11607143 & 2.26811953 \end{bmatrix}$$

b = the aerodynamic damping coefficients

$$\begin{bmatrix} (0.0461880214 & (0.0200148094 & (0.011423530 & 0.1026400 \\ +0.0078539816M) & -0.0019557637M) & +0.4218508.10^{-3}M) & \\ (0.0200148094 & (0.008775724 & (0.0050482849 & (0.0472144 \\ -0.0030029613M) & +0.0006021655M) & -0.3068996.10^{-3}M) & -0.164224.10^{-3}M) \\ (0.0114235294 & (0.0050482849 & (0.0029191367 & (0.0280140 \\ +0.0013350070M) & -0.0004508294M) & +0.0696282.10^{-3}M) & -0.161034.10^{-3}M) \\ 0.1026400 & (0.0472144 & (0.0280140 & 0.5474136 \\ & -0.164224.10^{-3}M) & -0.161034.10^{-3}M) & \end{bmatrix}$$

c = the aerodynamic stiffness coefficients

$$\begin{bmatrix} 0 & (0.0461880214M + 0.0078539816M^2) & (0.0444883026M - 0.00632056\,30M^2) & 0 \\ 0 & (0.0200148094M - 0.0030029613M^2) & (0.01936694\,3M + 0.0021637974M^2) & 0 \\ 0 & (0.0114235294M + 0.0013350070M^2) & (0.0110845603M - 0.0013247763M^2) & 0 \\ 0 & 0.1026400M & (0.1010916M - 0.91777.10^{-4}M^2) & 0 \end{bmatrix}$$

e = the structural stiffness coefficients

$$\begin{bmatrix} 0 & & \\ & 0 & \\ & & x \\ & & & y \end{bmatrix}$$

TABLE 4

Normal mode with wing bending (from quaternary).
Binary flutter calculation

$$
= \begin{vmatrix}
0.1578064441\ \lambda^2 & & 0.068229071\ \lambda^2 \\
+(0.9334318.10^{-3} & -0.2861794.10^{-4}M)\ \lambda & +(0.0164671908\ -0.16103529.10^{-3}M)\ \lambda \\
+(0.0060797493M & -0.61368159.10^{-3}M^2) & \\
+\ x & & \\
 & & \\
0.06229071\ \lambda^2 & & 2.26811953\ \lambda^2 \\
+(0.0164671908 & -0.16103529.10^{-3}M)\ \lambda & +0.5474136\ \lambda \\
+(0.101092405M & -0.91777.10^{-4}M^2) & +y
\end{vmatrix}
$$

TABLE 5

2 normal modes and wing bending (from quinary).
Ternary flutter calculation for M = 5

$$
= \begin{bmatrix}
0.15780637\,\lambda^2 & -0.6007.10^{-6}\,\lambda^2 & 0.06822828\,\lambda^2 \\
+0.79032796.10^{-3}\,\lambda & -0.006481885\,\lambda & +0.01566183\,\lambda \\
+0.015055308 & +0.3696417 & \\
+x & & \\
\\
-0.6007.10^{-6}\,\lambda^2 & 27.55985\,\lambda^2 & 0.71355033\,\lambda^2 \\
-0.01348681\,\lambda & +0.6692518\,\lambda & -0.18738398\,\lambda \\
-0.42822044 & +8.631057 & \\
 & +1428.57\,x & \\
\\
0.06822828\,\lambda^2 & 0.71355033\,\lambda^2 & 2.2681196\,\lambda^2 \\
+0.01566183\,\lambda & -0.18738398\,\lambda & +0.5474136\,\lambda \\
+0.50316358 & +3.230382 & +y
\end{bmatrix}
$$

Printed in England for Her Majesty's Stationery Office by the Royal Aircraft Establishment, Farnborough. W.T.60 K.4.

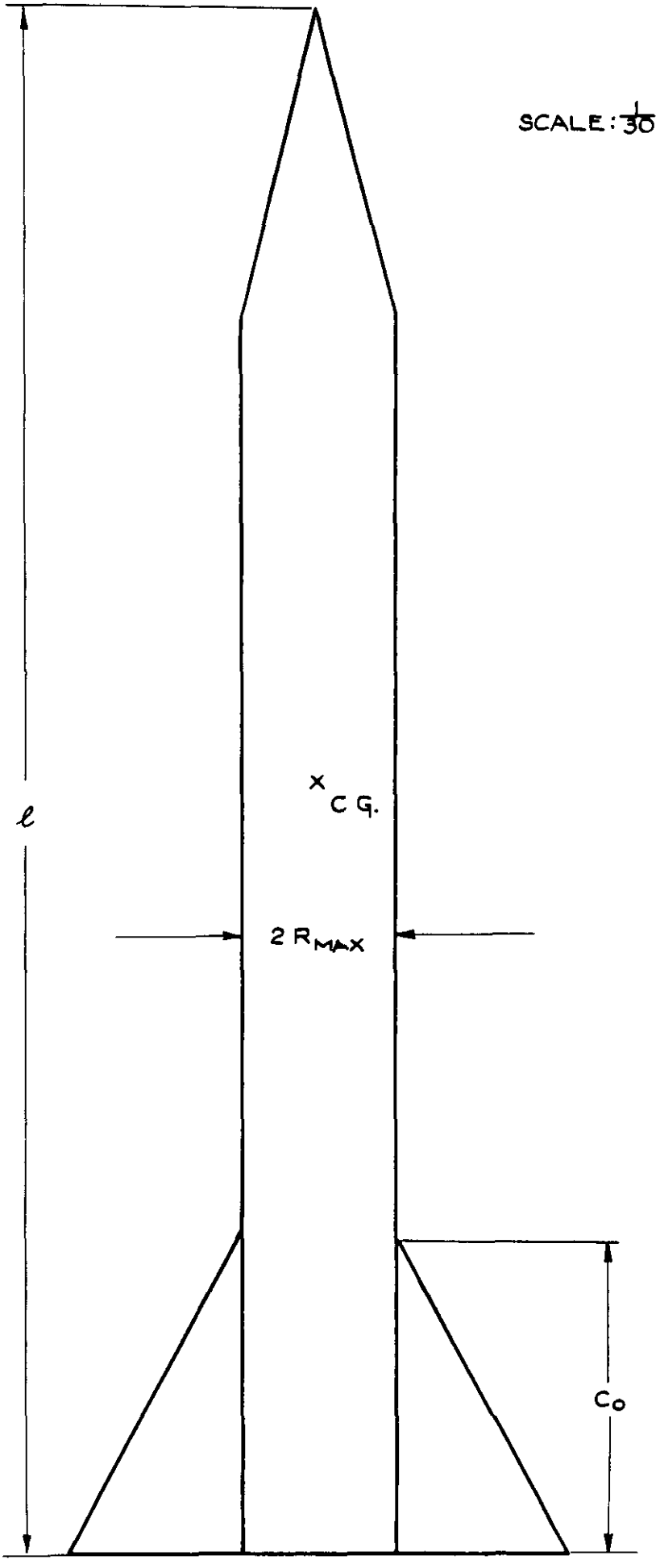

FIG. 1. PLAN VIEW OF CONFIGURATION CHOSEN.

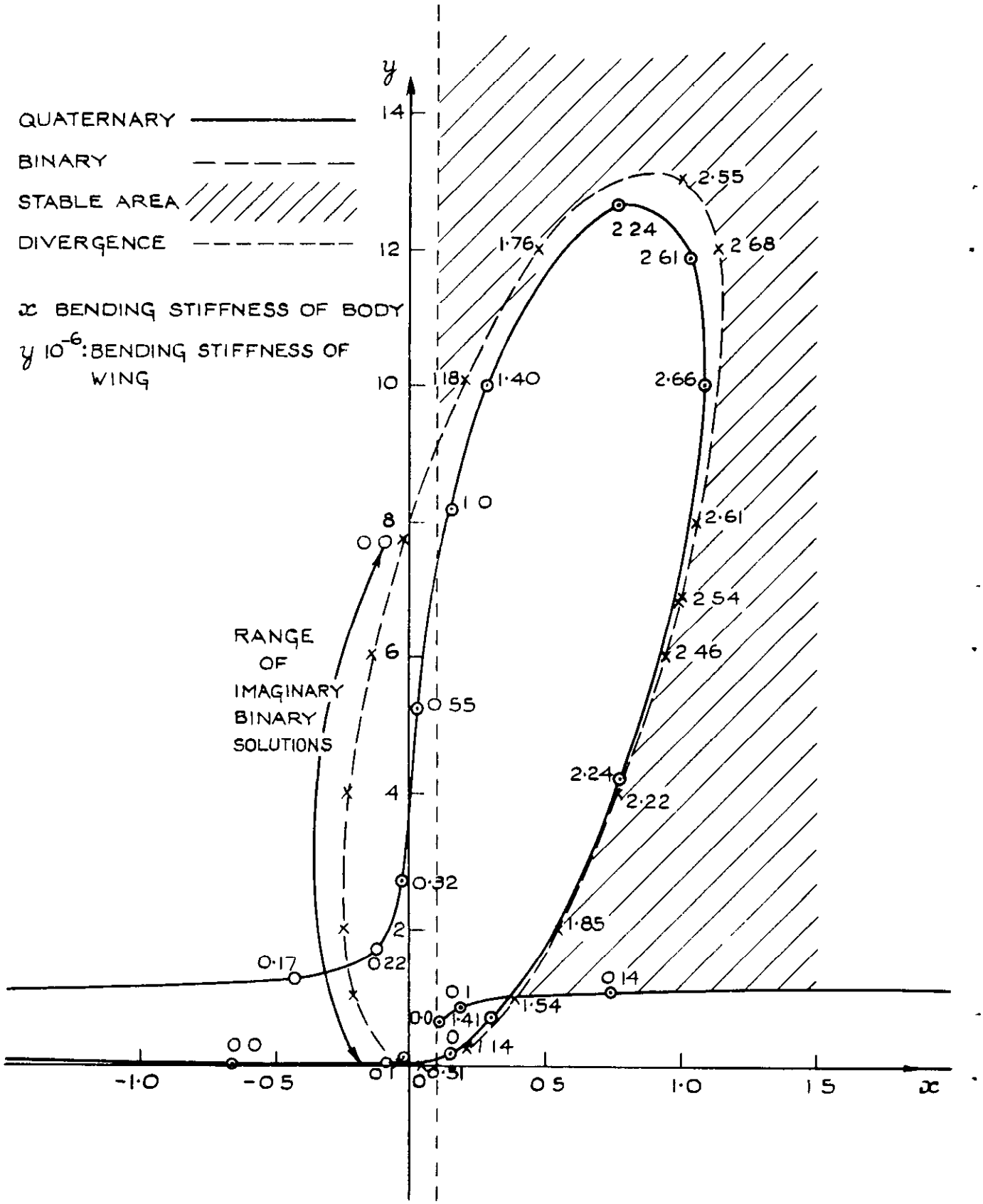

FIG. 2. TYPICAL FLUTTER BOUNDARY (M = 4) AND COMPARISON WITH A BINARY RESULT.

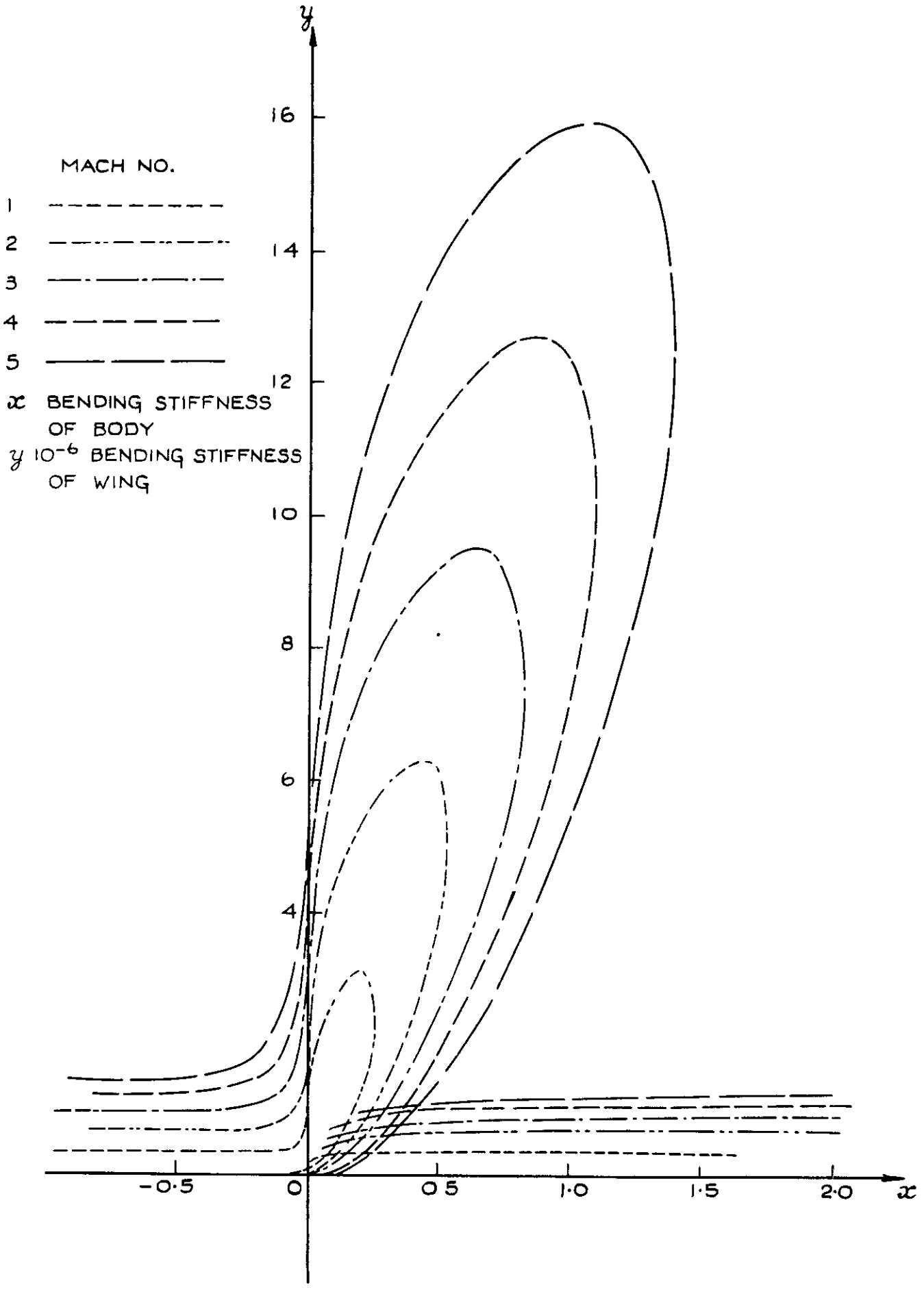

FIG.3. FLUTTER BOUNDARIES FOR 5 MACH NUMBERS.

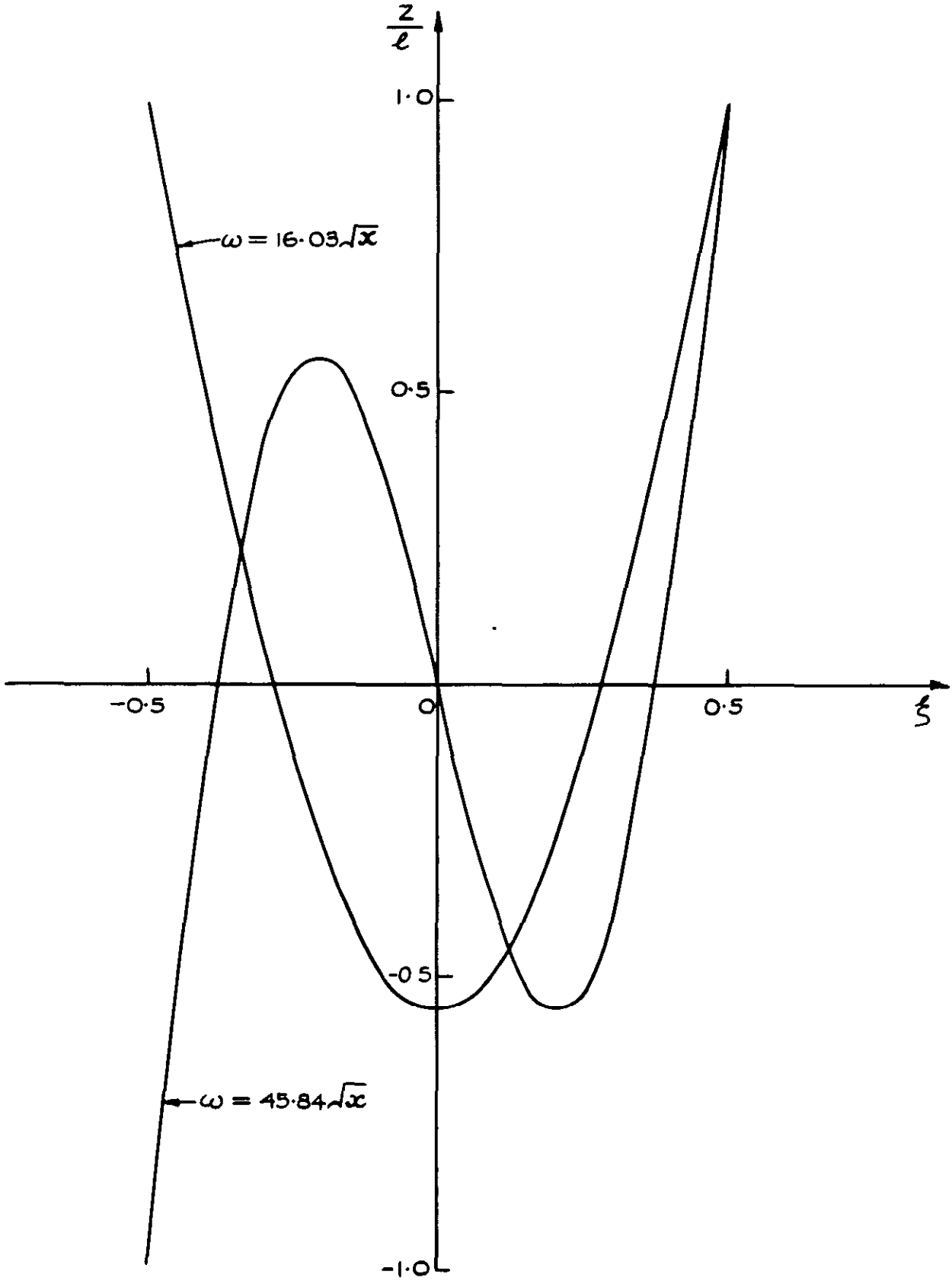

FIG. 4. THE FIRST TWO NORMAL MODES OF THE BODY.

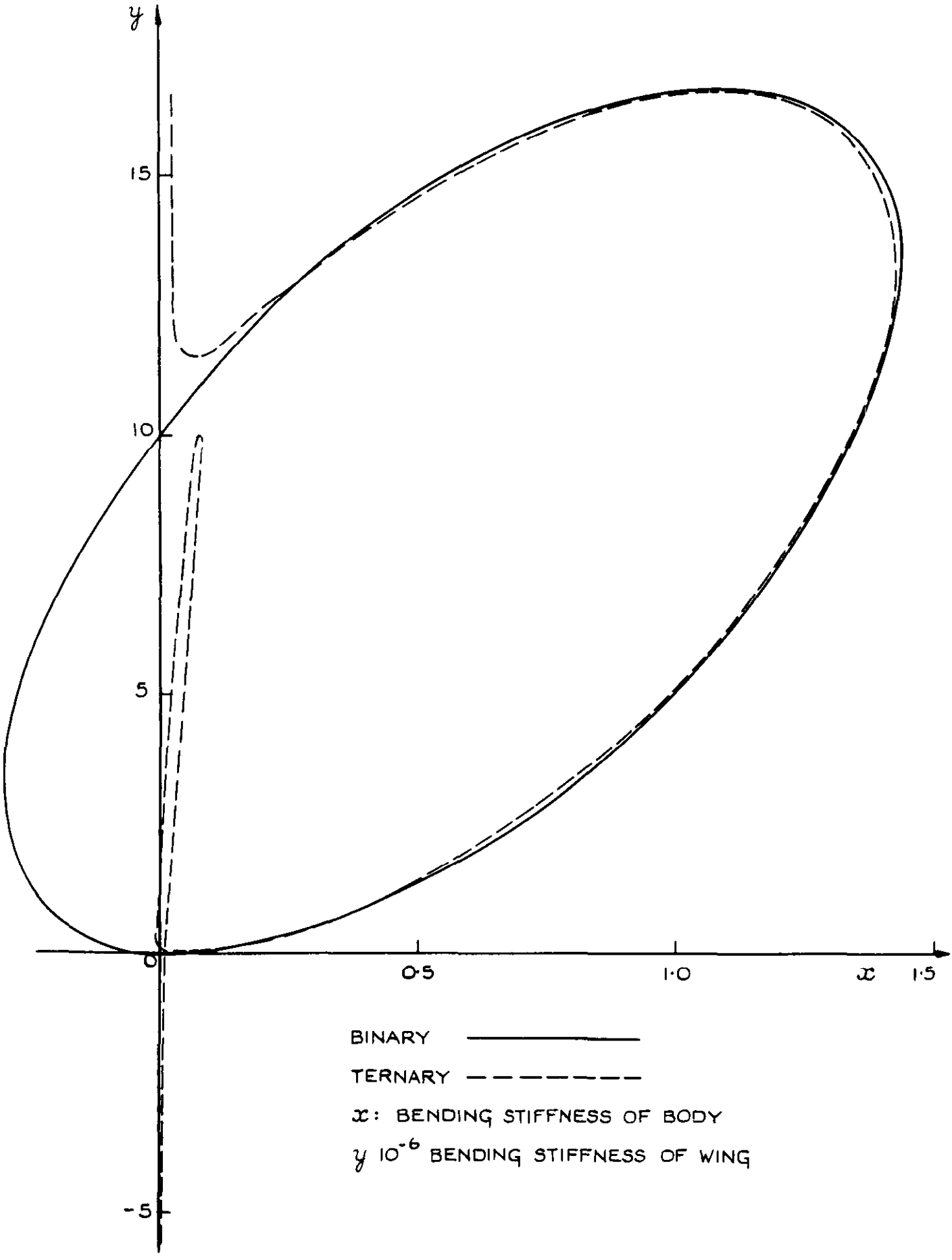

FIG. 5. EFFECT OF THE SECOND BODY MODE ON THE BINARY FLUTTER BOUNDARY (M=5)

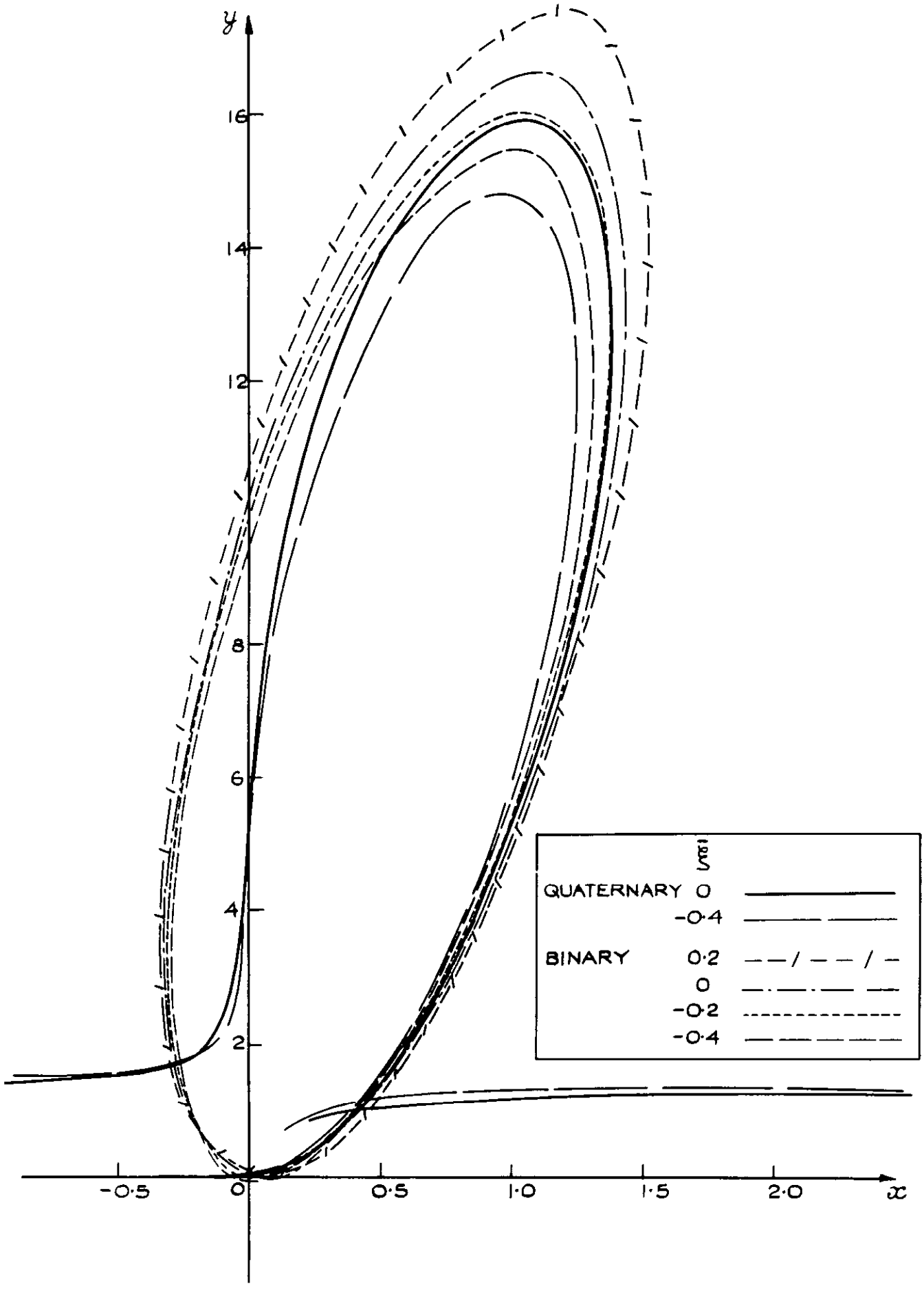

FIG. 6. EFFECT OF C.G. VARIATIONS ON THE FLUTTER BOUNDARIES (M = 5)

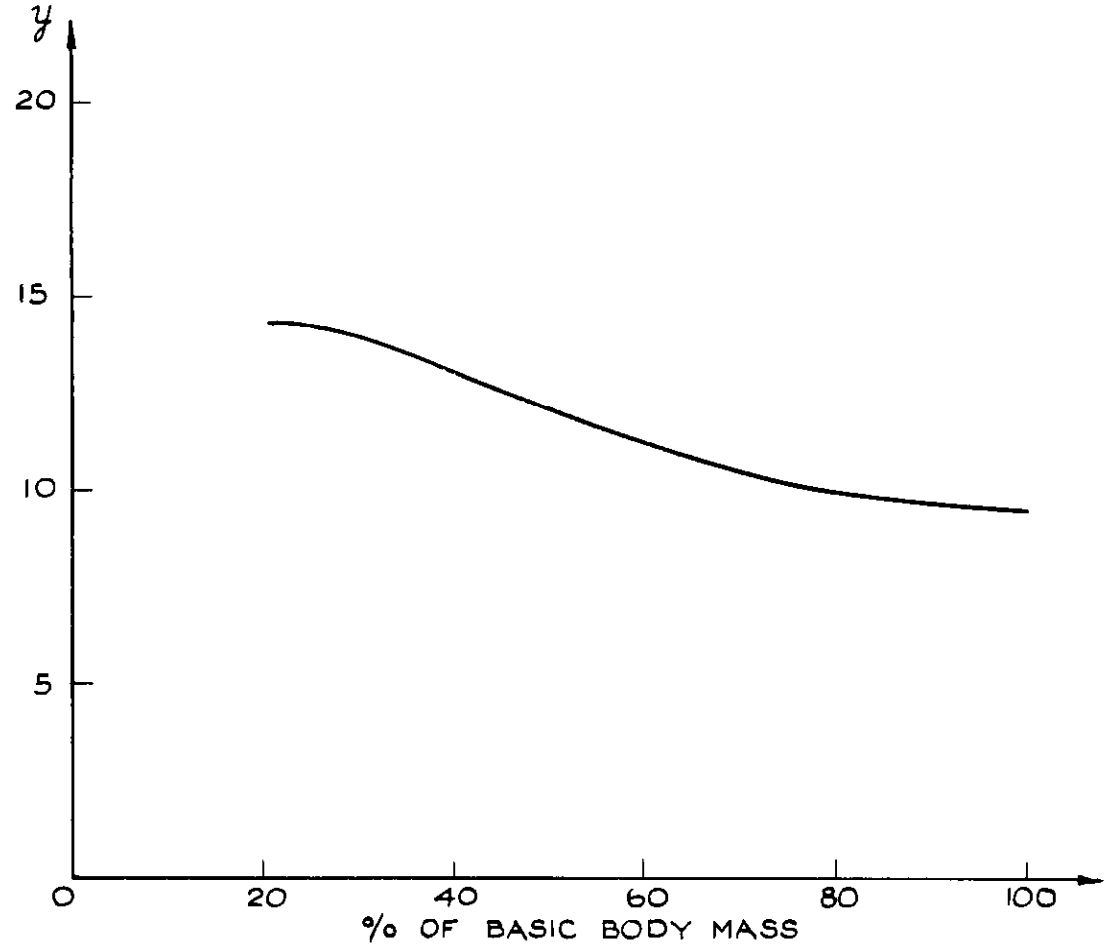

FIG.7. EFFECT OF BODY MASS ON THE FLUTTER BOUNDARIES ($x = 0{\cdot}14$)

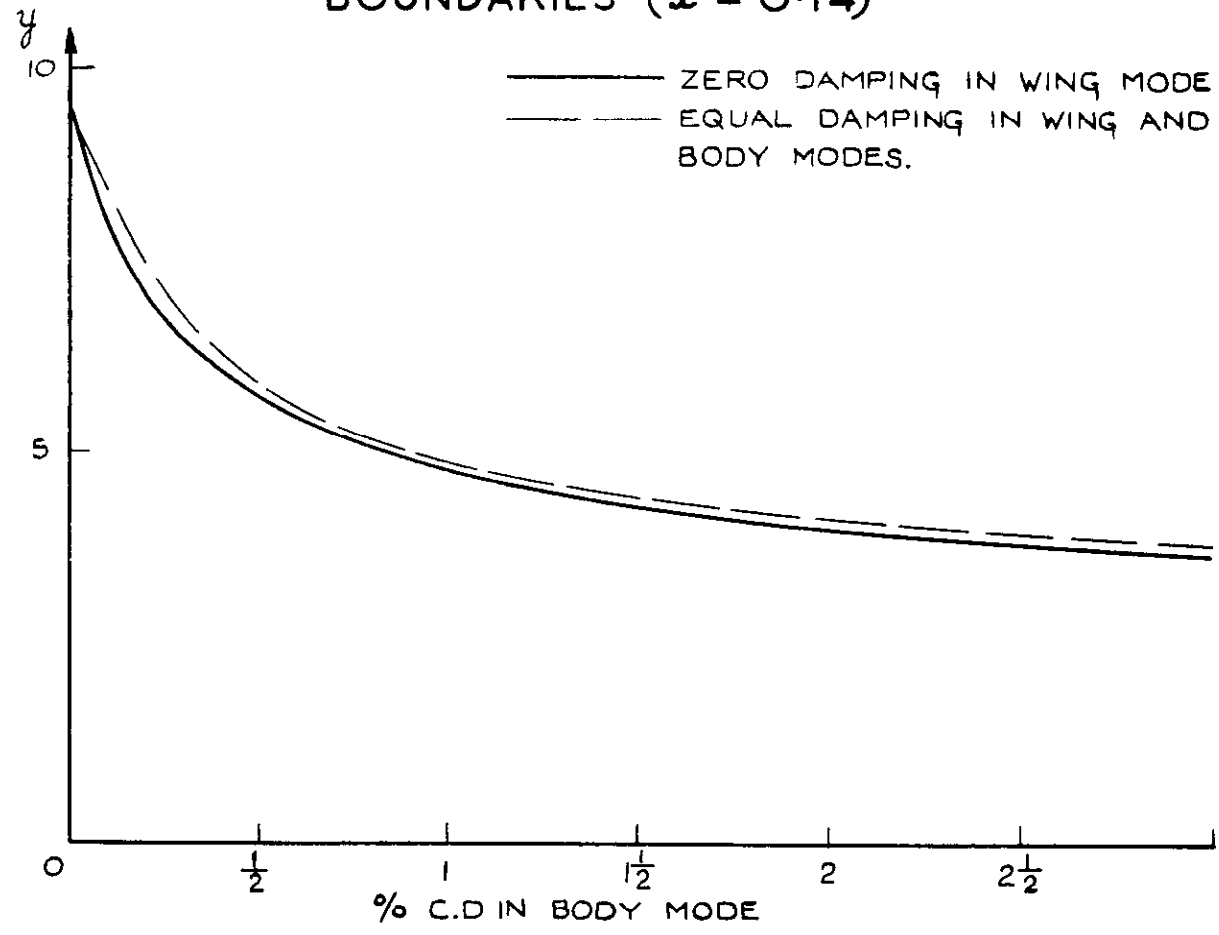

FIG.8. EFFECT OF STRUCTURAL DAMPING ON THE FLUTTER BOUNDARIES ($x = 0{\cdot}14$)

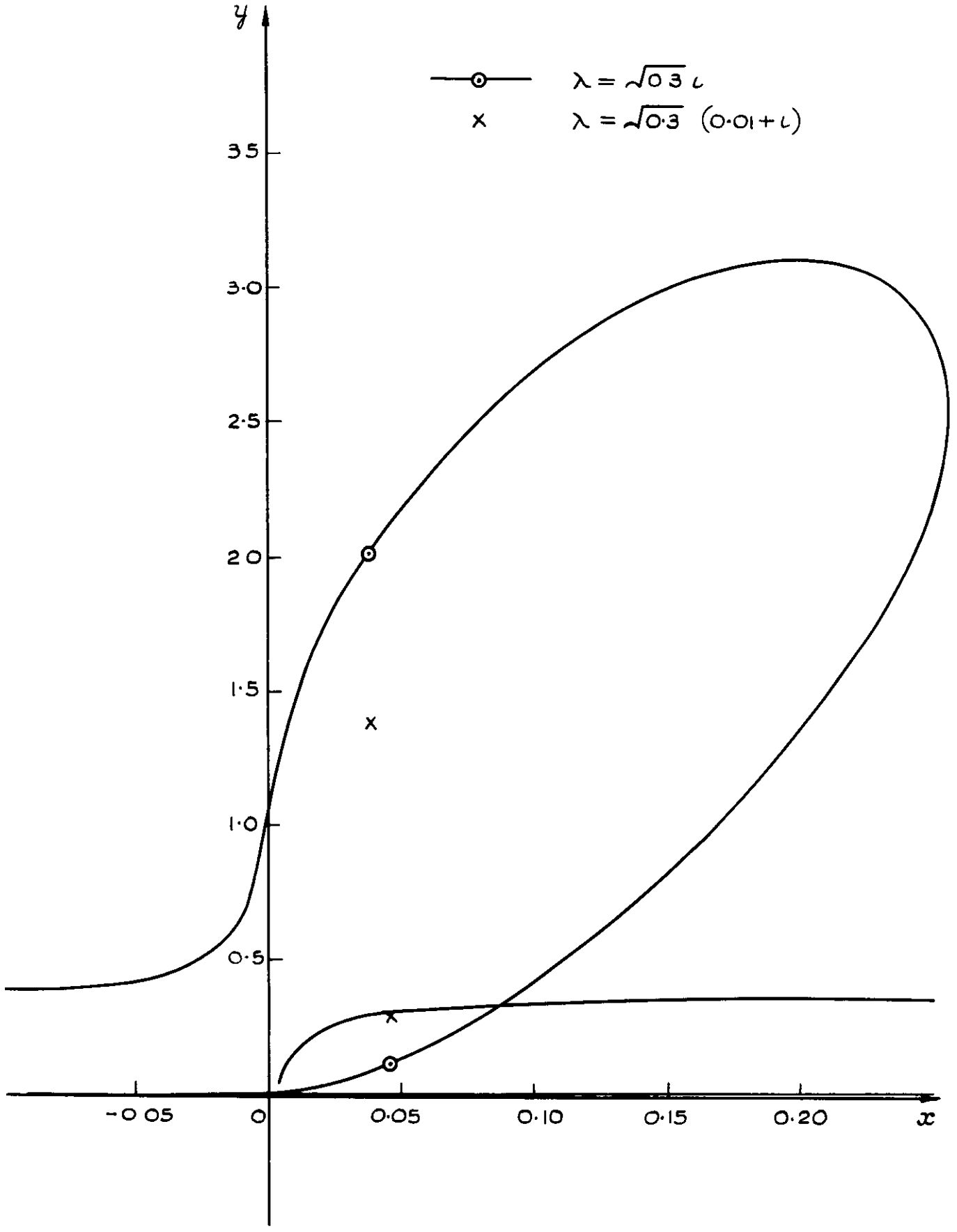

FIG. 9. TYPICAL FLUTTER BOUNDARY SHOWING TWO POINTS OF KNOWN INSTABILITY (M = 1)

A.R.C. C.P. No.761

533.6.013.422 : 629.19.012.674

FLUTTER CALCULATIONS ON A BODY WITH AFT WINGS.
Broadbent, E.G. and Hartley, E.V. August, 1963.

The effect of body flexibility on the flutter of a body with aft wings is investigated. The missile is in free supersonic flight and the wings are assumed rigid in torsion. It is found that flutter can occur either between wing bending and the rigid body modes, or between wing bending and the fundamental bending mode of the body, depending on body stiffness. If the latter form of flutter is possible (as it usually is in practice) a higher wing stiffness is required for its avoidance. A close approximation to the quaternary flutter solution in this case is given by the appropriate binary calculation. The flutter is fairly sensitive to parameters that affect the static margin (Mach number and c.g. position) and also to structural damping.

A.R.C. C.P. No.761

533.6.013.422 : 629.19.012.674

FLUTTER CALCULATIONS ON A BODY WITH AFT WINGS.
Broadbent, E.G. and Hartley, E.V. August, 1963.

The effect of body flexibility on the flutter of a body with aft wings is investigated. The missile is in free supersonic flight and the wings are assumed rigid in torsion. It is found that flutter can occur either between wing bending and the rigid body modes, or between wing bending and the fundamental bending mode of the body, depending on body stiffness. If the latter form of flutter is possible (as it usually is in practice) a higher wing stiffness is required for its avoidance. A close approximation to the quaternary flutter solution in this case is given by the appropriate binary calculation. The flutter is fairly sensitive to parameters that affect the static margin (Mach number and c.g. position) and also to structural damping.

A.R.C. C.P. No.761

533.6.013.422 : 629.19.012.674

FLUTTER CALCULATIONS ON A BODY WITH AFT WINGS.
Broadbent, E.G. and Hartley, E.V. August, 1963.

The effect of body flexibility on the flutter of a body with aft wings is investigated. The missile is in free supersonic flight and the wings are assumed rigid in torsion. It is found that flutter can occur either between wing bending and the rigid body modes, or between wing bending and the fundamental bending mode of the body, depending on body stiffness. If the latter form of flutter is possible (as it usually is in practice) a higher wing stiffness is required for its avoidance. A close approximation to the quaternary flutter solution in this case is given by the appropriate binary calculation. The flutter is fairly sensitive to parameters that affect the static margin (Mach number and c.g. position) and also to structural damping.

Published by
HER MAJESTY'S STATIONERY OFFICE

To be purchased from
York House, Kingsway, London w.c.2
423 Oxford Street, London w.1
13A Castle Street, Edinburgh 2
109 St Mary Street, Cardiff
39 King Street, Manchester 2
50 Fairfax Street, Bristol 1
35 Smallbrook, Ringway, Birmingham 5
80 Chichester Street, Belfast 1
or through any bookseller

C.P. No. 761

S.O. CODE No 23-9015-61